Comparison between a Uniaxial Compaction Tester and a Shear Tester for the Characterization of Powder Flowability[†]

Luca Parrella[1,3], Diego Barletta[1], Renee Boerefijn[2] and Massimo Poletto[1*]
Dipartimento di Ingegneria Chimica e Alimentare, Università degli Studi di Salerno[1]
Purac Biochem bv[2]

Abstract

The complete characterization of powder flow properties with shear cells is a long and time-consuming process that requires specially trained operators or costly automated instruments. For these reasons, in industrial practice, the use of simpler and less extensive measurement by uniaxial compaction testers is often preferred. However, previous studies in the literature indicate that the results of the two techniques are not directly comparable due to the different stress state conditions achieved in the two testers.

In this study, an experimental campaign to measure the flow function of five different powders with a ring shear tester (RST) and a uniaxial compaction tester (UCT) was performed. Different flowability results that arose for the more cohesive powders are explained by the wall friction effect in the UCT. Re-evaluation of the results accounting for the wall friction gave substantial agreement between the two experimental techniques for a calcium carbonate powder and only at low consolidation levels for the other four food powders. Phenomena other than wall friction seem to appear within these powders tested at high consolidation levels. The comparison between the results of the two techniques suggests that straightforward extrapolation of the UCT flow functions to a low consolidation condition can lead to an underestimation of powder cohesion.

Keywords: powder flowability, uniaxial compaction tester, ring shear tester, wall friction, cohesive powders

1. Introduction

The flow properties of bulk solids are key properties in the design and control for storage and handling operations in several industrial applications. Powder flowability is usually expressed in terms of flow functions which represent the unconfined yield strength, f_c, of the material as a function of the major principal stress at steady state, σ_1. The ratio between the two is referred to as the flow factor $ff_c = \sigma_1/f_c$ and is used as a flowability index according to the classification by Jenike (1961). This classification was extended by Tomas and Schubert (1979) and classifies the powder's behaviour as follows: $ff_c \leq 1$ hardened, $1 < ff_c \leq 2$ very cohesive, $2 < ff_c \leq 4$ cohesive, $4 < ff_c$ ≤ 10 easy flowing, $ff_c > 10$ free-flowing. After the pioneering work of Jenike (1961), a variety of different experimental techniques were developed over four decades to experimentally characterize the powder flow functions, as reported in recent comprehensive surveys by Schwedes (2003) and by Schulze (2008). All these testers are divided into two main categories: direct and indirect testers. In the first category, the shear region is directionally forced onto the powder sample, while in the second, this region is thought to develop independently of the tester geometry. Shear cells, from the first translational model developed by Jenike (1961) to the more recent rotational model developed by Schulze (1994), are so-called direct testers. In these testers, in fact, a shear force induces the formation of a shear region in the powder specimen consolidated by a normal force. Shear cells are widely used both for fundamental research and for industrial testing, e.g. in silo design. For this latter application, in particular, shear test methods different from shear cells are used, such as uniaxial compaction testers. In these testers, the bulk solids are com-

pacted in a cylindrical mould exerting some consolidation by means of a moving plunger or piston, then the mould is removed and the force necessary to break the sample, acting in the same direction of the compaction force, is measured. These are so-called indirect testers because shear regions are thought to develop along directions other than normal to the force. Several studies (Williams et al., 1971; Gerritsen, 1986; Maltby and Enstad, 1993) report that the main limitation of this technique is that a minimum consolidation stress on the powder sample is necessary to avoid its failure under gravity alone just after removing the mould. This minimum consolidation stress value is larger than the value that can be attained in shear cell tests and might be considerably larger than the stress acting within small process hoppers. In practice, this means that the powder compaction under its own weight is completely negligible, but cohesion forces may still cause flowability problems. Nevertheless, the uniaxial compression test is often preferred in industrial practice due to its simplicity and to the shorter time necessary to characterize the powder flowability, either in terms of a single unconfined yield strength for a single consolidation force, or in terms of a complete flow function. A recent example of this shear testing practice is given by Zhong et al. (2000), whose application to the classification of powder flowability was tested by Bell et al. (2007). Unfortunately, the comparison between the powder strength values measured by the two techniques is not straightforward. In fact, experimental results obtained with a biaxial tester by Schwedes and Schulze (1990) suggest that the powder specimen follows different stress histories in a shear tester and in a uniaxial tester during the consolidation step. In the first case, the powder sample finally attains steady state deformation, which means deformation without bulk density variation. In the second, it was not possible to achieve this condition due to the lateral confinement of the sample by the mould walls. As a result, the final consolidation states achievable by the two techniques could be different. A major difference between uniaxial compression tests and annular/linear shear tests is the role of friction exerted by the mould wall on the powder sample. This wall friction supports part of the external vertical force applied on the powder specimen for consolidation. By applying a simple balance of forces on a differential slice element of the powder under compression in the mould (in the style of Janssen as reported by Nedderman, 1992), we obtained the well-known equation for the effective normal stress σ in cylinders containing powders subject to their weight and to some external vertical load on the upper surface:

$$\sigma = \sigma_0 \exp\left(-\frac{4\mu_w K z}{D}\right) + \frac{\rho_b g D}{4\mu_w K}\left[1 - \exp\left(-\frac{4\mu_w K z}{D}\right)\right] \quad (1)$$

where σ_0 is the surcharge stress due to the external vertical force on the top surface, μ_w is the wall friction coefficient, K is the ratio between the radial and the vertical principal stresses, z is the vertical coordinate oriented downwards, D is the mould diameter, ρ_b is the powder bulk density and g is the acceleration due to gravity. Uniaxial compression tests are usually performed at high consolidation stresses, and the second term of equation (1) due to the powder weight can be neglected. Therefore, the resulting normal stress decreases exponentially over the powder sample depth.

Some effort to overcome the wall friction effect was pursued by Williams et al. (1971), who repeated the experiment by preparing powder samples obtained with the subsequent compaction of an increasing number of thin layers. They derived the unconfined yield strength from the measured values of sample yield strength extrapolated to an infinite number of layers. Maltby and Enstad (1993) tried to eliminate the wall friction problem by wrapping the powder sample in a flexible membrane and applying a lubricating oil between the membrane and the mould wall. Both the flow functions obtained by uniaxial compression tests by Williams et al. (1971) and by Maltby and Enstad (1993) are very close to those derived from Jenike shear cell experiments, suggesting that wall friction is perhaps the main cause of differences between rotational/translational shear testers and uniaxial compression test results. Unfortunately, the procedures proposed to avoid the wall friction effect with their complications risk annulment of the intrinsic simplicity of the uniaxial compression tests and are therefore not pursued in industrial practice.

The scope of this work is to compare uniaxial compression tests and shear cell tests for a number of food powders of different cohesion classes and for a reference calcium carbonate powder. In particular, going by experimental evidence reported in the literature, it is expected that uniaxial testing will provide apparent powder flowability that is higher than that evaluated with shear testing. An attempt will be made to account for the main causes of these discrepancies in order to reconcile the powder flowabilities obtained with the different techniques.

2. Experimental Set-Up

2.1 Apparatus

Three different testers for measuring the flow properties of bulk solids were used in this study: a uniaxial compaction tester and a Schulze ring shear tester (1994) to measure the powder flow functions, and a Peschl rotational shear tester (1989) to measure the angle of wall friction.

The uniaxial compaction tester (UCT) consists of a PVC cylindrical mould axially split into two halves. The cylinder (92.5 mm ID and 120 mm high) is secured by a chain-clamp to a thin disc fixed on to the horizontal base and a second disc is placed as the lid on the top surface of the powder sample in the mould. A piston moving downwards by means of an electrically driven motor applies a normal force to the lid over the specimen. This force is measured by a load cell.

The Schulze ring shear tester (RST) used in this study is the manually operated commercial version. Two different annular cells were used: the standard M cell with an internal volume of about 940 cm^3, and the smaller SV10 cell with an internal volume of about 96 cm^3. Normal loads were applied to the hanger hooked onto the lid of the cell. The shear force acting during the experiments was derived from the torque measured by the load cells connected to the cover through the tie rods. The powder sample volume was measured by a linear displacement transducer connected to the cell lid.

The rotational shear tester of Peschl was used to measure the wall yield loci of the powders. To this end, a wall sample was fixed to the cell base by three radial screws. A ring was centred on the wall sample and filled with the powder specimen. External loads were applied directly to the cylinder attached to the lid over the specimen top surface. The shear force was derived from the torque measured by a load cell connected to the lid through a rod.

2.2 Materials

Five different powders were tested. A calcium carbonate powder was used as a reference material. The other four powders, provided by PURAC Biochem, were used in this study to span the full range of flowability classes. For confidentiality reasons, we will refer to these as powders A, B, C and D. The volumetric particle size distribution of each powder was measured by a Malvern Mastersizer 2000 laser diffraction analyser on powder samples dispersed in a non-solvent liquid. The results in terms of median particle size d_{50}, Sauter mean size d_{32} and size range corresponding to 80% of the distribution are reported in **Table 1**. Scanning electron micrographs of materials shown in **Fig. 1** reveal that the calcium carbonate powder and powders A and B consist of irregular flaky particles while powders C and D show a more rounded shape. The aerated bulk density and tapped bulk density and therefore their ratio referred to as the Hausner ratio were measured by a Hosokawa tester. The angle of repose φ_r was also determined by a Hosokawa tester. All these results are reported in **Table 1**.

Under strict application of the Mohr-Coulomb analysis, the values of K appearing in Equation (1) can be calculated according to Rankine equation:

$$K = \frac{1 - \sin \varphi_e}{1 + \sin \varphi_e} \tag{2}$$

where φ_e is the effective angle of friction measured with the RST. Values of K calculated with equation (5) are reported in **Table 1**. These values fall in the range between 0.1 and 0.27. Instead, direct measurements of K reported by Kwade et al. (1994) show that K values are generally between 0.4 and 0.6 also for cohesive powders. Therefore, to avoid errors arising from an underestimation of K, its value was set to 0.4 for all the powders tested. The wall friction angle φ_w was derived from the wall yield loci measured with a Peschl shear tester on a wall sample of the same material which the UCT mould is made of.

### 2.3 Procedures

2.3.1 Uniaxial compression test procedure

Once the cylindrical mould is filled with the pow-

Table 1 Material properties

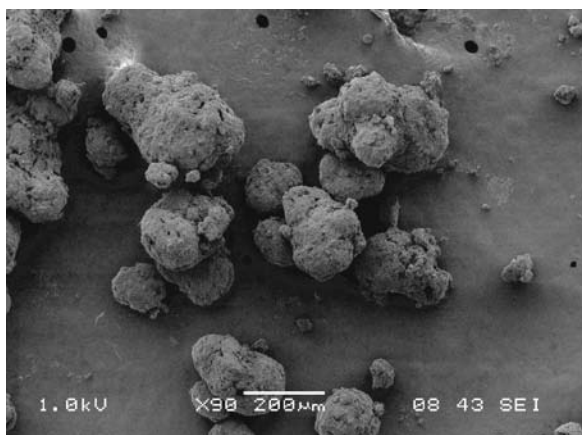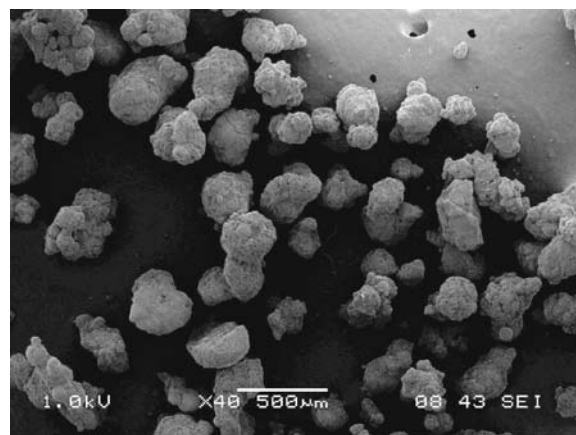| Material	d_{50} μm	80% range μm	d_{32} μm	aerated ρ_b kg m^{-3}	tapped ρ_b kg m^{-3}	CI %	ϕ_r deg	ϕ_e deg	ϕ_w deg	K eq (9)	Jenike (1961) flowability UCT corrected
CaCO₃	7	2-40	4	336	421	20.2	45	54	22	0.10	Cohesive
A	25	1-246	4	434	910	52.3	48	49	25	0.14	Cohesive
B	3	1-32	2	242	595	59.4	48	55	31	0.099	Very cohesive
C	267	149-467	221	610	667	8.6	37	47	26	0.16	Cohesive
D	198	82-386	117	688	706	2.6	32	35	12	0.27	Free flowing
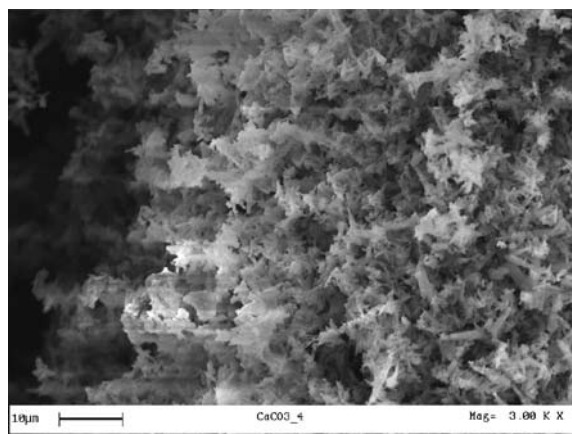
CaCO$_3$
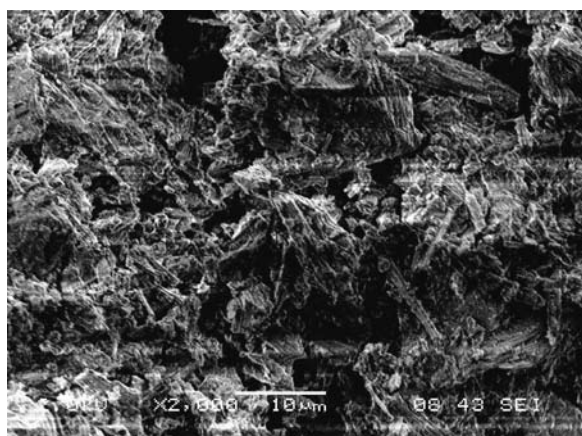
A
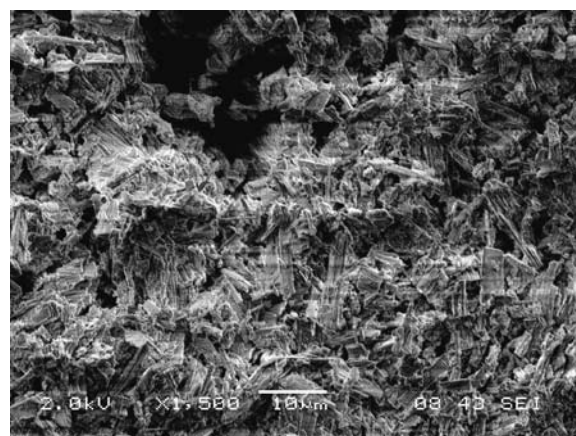
B

C

D

Fig. 1 SEM micrographs of the materials used.

der specimen and the top lid is placed on its surface, the consolidation step is performed by moving the piston downwards and applying the desired normal load, N_c. Then the piston moves upwards, releasing the consolidation force. The mould is opened and removed carefully in order not to disturb the consolidated specimen. The compression step is carried out by moving the piston downwards onto the powder sample with increasing normal force until the specimen fails. From this test, a single f_c-σ_1 point of the flow function can be derived as follows:

$$\sigma_1 = \frac{N_c}{A_{UCT}} \tag{3}$$

$$f_c = \frac{N_f}{A_{UCT}} \qquad (4)$$

where A_{UCT} is the cross-sectional area of the cylindrical mould and N_f is the normal force measured at failure. By repeating the whole procedure with different consolidation normal loads, a complete flow function is obtained.

A second procedure was used to account for wall friction. In particular, σ_1 was evaluated according to Equation (1), assuming z to be equal to the measured powder sample height after consolidation. The underlying hypothesis is that in the UCT, the compaction strength changes within the sample and, in particular, that the smaller consolidation, which determines the failure load, is attained at the sample bottom. In the same way, the unconfined yield strength f_c was also calculated by accounting for the contribution caused by the powder sample weight, M, as follows:

$$f_c = \frac{N_f + M}{A_{UCT}} \qquad (5)$$

2.3.2 Ring shear test procedure

The standard measurement procedure was followed to measure a yield locus with a Schulze RST. According to this procedure, once the shear cell with the powder specimen has been prepared and the maximum normal load chosen, N_c, is applied to the cell lid. The pre-shearing step starts and is carried out up to attainment of a steady state value of the shear stress, τ. Then the shearing phase takes place under a normal load, N_1, lower than N_c, to reach a peak value of shear stress corresponding to the incipient flow of the material. The sequence of the two steps is repeated with the same N_c for each pre-shearing phase, but with decreasing normal loads for each shearing phase (i.e. $N_1 > N_2 > \cdots > N_n$). A qualitative sketch of a typical shear stress chart achievable during a shear test is reported in **Fig. 2**. In this work at least five failure points were measured for the construction of each yield locus and each complete test was repeated twice.

The normal stress σ acting on the shear plane in a failure test is calculated as follows:

$$\sigma = \frac{N}{A_{RST}} + \rho_b g \Delta z \qquad (6)$$

where N is the external normal load applied, A_{RST} is the cell cross-sectional area and Δz is the powder height over the shear plane. The average shear stress τ acting on the shear plane is derived from the measured torque. The σ-τ points obtained at failure are reported in a plot to derive the powder static yield locus corresponding to the consolidation applied in the test as sketched in **Fig. 3**. In addition to these points, the average of the steady state σ-τ values
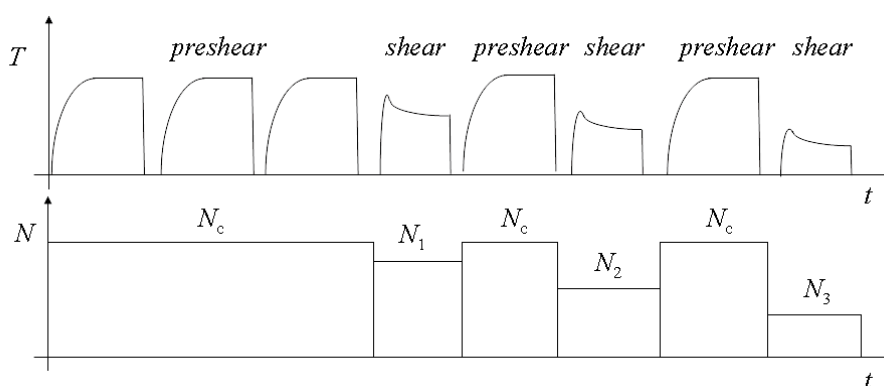

Fig. 2 Typical torque and normal load chart during a shear cell experiment.
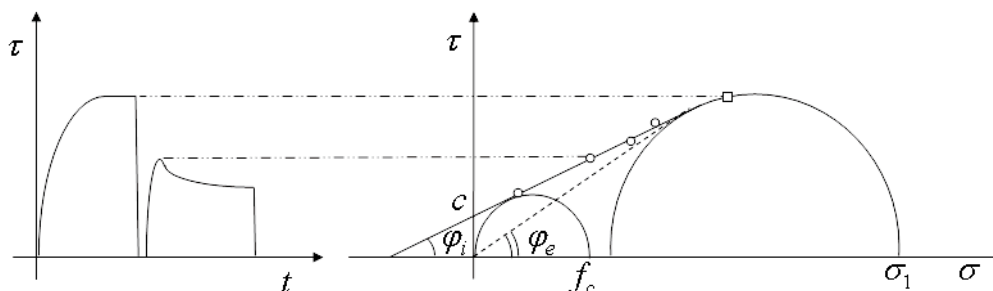

Fig. 3 Yield locus construction from shear experiment data.

obtained during the pre-shearing steps is reported on the same diagram. The Mohr circle drawn through the steady state point and tangent to the yield locus locates the major principle stress σ_1 corresponding to the consolidation applied. The unconfined yield strength of the powder f_c is given by the major principle stress of the Mohr circle through the origin and tangent to the yield locus. The angle φ_i between the static yield locus and the σ axis is the static angle of internal friction. The dashed line passing through the origin and tangent to the larger Mohr circle is the effective yield locus. Its angle of inclination with respect to the σ axis is the effective angle of friction, φ_e. By performing other complete shear tests at different N_c values, a complete flow function of the powder can be plotted.

2.3.3 Wall friction measurement procedure

The wall friction coefficient between the powder and the mould material was evaluated with the Peschl shear tester. The detailed procedure is as follows: after the ring placed on the wall sample has been filled with the powder, a normal load N_1 is applied to the cell lid and the shearing takes place until a steady state value of τ is measured; this step is repeated consecutively three times to be sure that critical consolidation of the powder has been reached under the applied load; this sequence is then repeated with the same sample by applying increasing normal loads (i.e. $N_1 < N_2 < \cdots < N_n$). Normal and shear stresses are calculated as in the Schulze RST, taking the different cell geometry into account. The σ-τ points are plotted to obtain the wall yield locus. The angle between

the wall yield locus and the σ axis is the angle of wall friction φ_w. The wall friction coefficient, μ_w, is the tangent of this angle.

3. Results

The flow functions measured for all the materials are reported in **Figs. 4-8**. In these figures, solid black circles and hollow circles with thick contours refer to experiments carried out on the M cell of the RST, whereas hollow circles refer to experiments carried out on the SV10 cell of the RST and squares refer to experiments carried out on the UCT. As previously mentioned, all experiments were repeated twice and showed a good reproducibility of data, and therefore deviations from expected trends, as discussed in the following, can be attributed to inherent experimental conditions. A general inspection of the figures reveals that the five materials investigated cover a wide range of flow behaviours evaluated according to the Jenike classification. From the distribution of flow data in the Jenike classification regions and the analysis of **Table 1**, it appears clear that a good correlation exists between the flow behaviour of the powder measured with RST and the powder compressibility index in **Table 1**. This is in agreement with what was reported by Santomaso et al. (2003). The only exception to this agreement was found for powder C. This singularity might probably be attributed to the very irregular and complex shape of these particles shown in **Fig. 1**.

The flow function for calcium carbonate (**Fig. 4**) obtained with the RST lays within the cohesive region
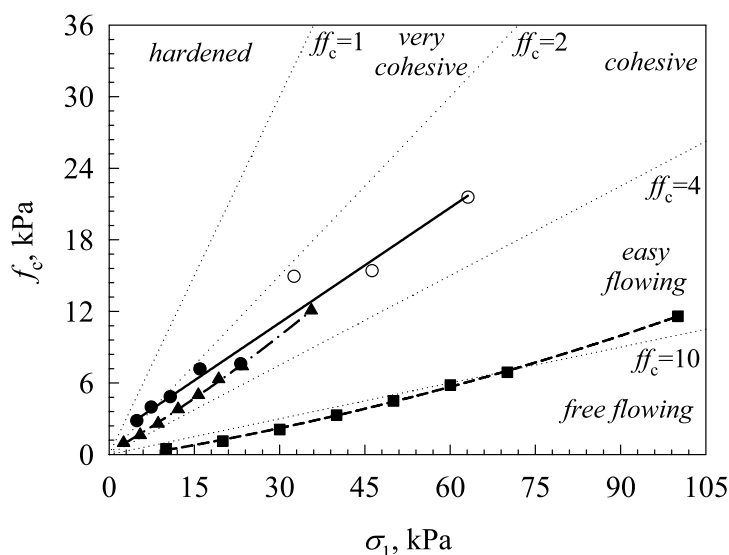

Fig. 4 Flow functions for calcium carbonate powder. ● RST M cell; ○, RST SV10 cell; ■, UCT; ▲, UCT corrected.

and tends to the very cohesive region at low consolidation. Both the M cell and the SV10 cell were used with the RST to cover a wider range of consolidation stresses. The UCT flow function is more linear and is located between the easy-flowing and free-flowing region.

The flow function for powder A (**Fig. 5**) obtained with the M cell of the RST crosses different regions of flow behaviour from very cohesive to easy flowing, showing an apparent better flowability as the major principal stress σ_1 increases. Significant time fluctuations typical of slip-stick behaviour were observed in shear stress charts of the experiments corresponding to $\sigma_1 > 5$ kPa. Since this phenomenon could lead to an incorrect estimation of the yield locus and consequently of the unconfined yield strength of the powder, this set of experiments was repeated with the smaller SV10 cell of the RST in which the slip-stick flow was not expected for the different elastic properties of the system due to the reduced height of the powder sample. As a result, the points derived from M cell tests, represented by hollow circles with thick contours, were discarded and, in the regression of the RST flow function (solid line), were substituted with the points obtained with the SV10 cell of the RST, which are reported as hollow circles. The RST flow function derived with this procedure shows a certain convexity and covers three different flowability regions. The flow function obtained with the UCT instead shows a linear increase of fc with increasing σ_1 and lies entirely in the easy-flowing region.

The flow function obtained for material B with the M cell RST (**Fig. 6**) follows a trend similar to that of powder A and extends over three different flowability regions (very cohesive, cohesive and easy flowing). Also in this case, the experiments for $\sigma_1 > 5$ kPa were repeated with the SV10 cell of the RST to better investigate the unexpected significant decrease of f_c values, which was not necessarily associated to slip-stick flow. The RST flow function curve resulting from the regression on filled circles and hollow circles with thin contours shows a high powder cohesion. Also in this case, the flow function derived from the UCT is a straight line and it falls in the region of cohesive powders. The corresponding f_c values are smaller than those measured with the RST for $\sigma_1 < 20$ kPa.

The flow function measurement for powder C with the M cell of the RST (**Fig. 7**) yielded a linear increase of f_c with increasing σ_1. All the flow function points belong to the cohesive region. Slip-stick flow was not observed for the whole range of investigated stress states, but additional experiments with the SV10 cell of RST were performed at high σ_1. Corresponding results confirmed the trend observed with the M cell. The flow function obtained with UCT is lower than the RST, suggesting an easy-flowing behaviour.

Powder D's flow function obtained with the M cell of RST (**Fig. 8**) is a straight line in the free-flowing region. Slip-stick behaviour was observed for $\sigma_1 > 10$ kPa, but the repeated tests with the SV10 cell RST gave identical f_c values. It was really difficult to perform the uniaxial compaction tests since the low cohesion of powder D allowed the preparation of stable powder specimens only at very high consolidation stresses. The resulting flow function coincides with that obtained with the RST.
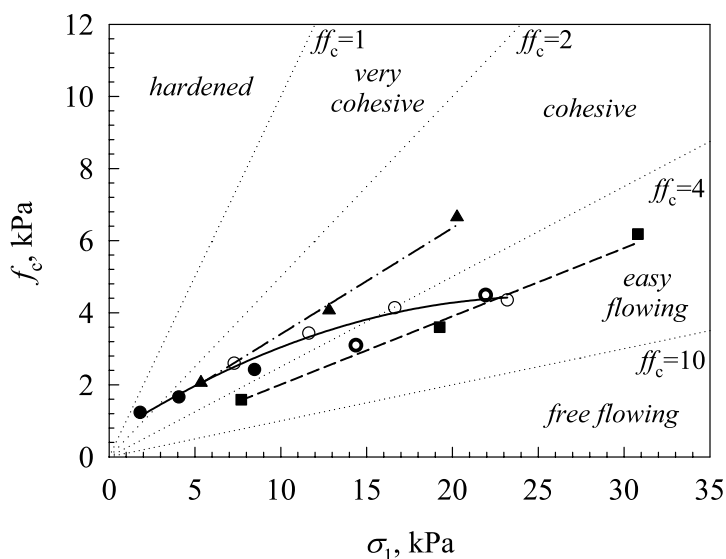
Fig. 5 Flow functions for powder A. ● ○ RST M cell; ○, RST SV10 cell; ■, UCT; ▲, UCT corrected.
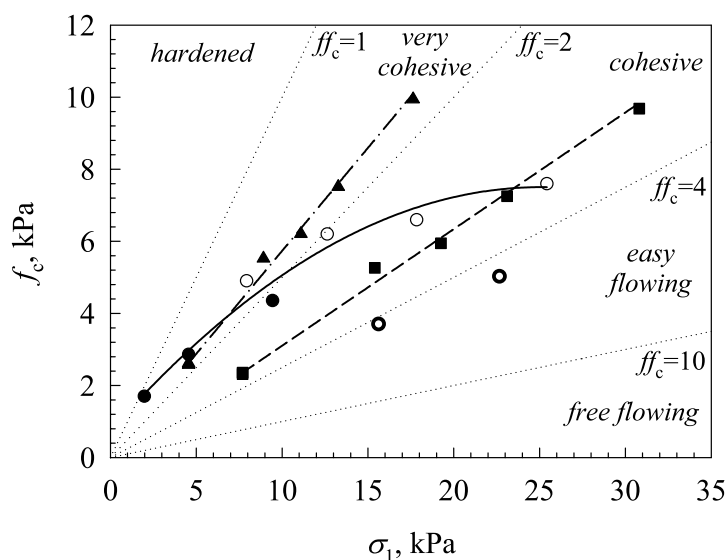
Fig. 6 Flow functions for powder B. ● ○RST M cell; ○, RST SV10 cell; ■, ideal UCT eqs. (1) and (2); ▲, UCT corrected.
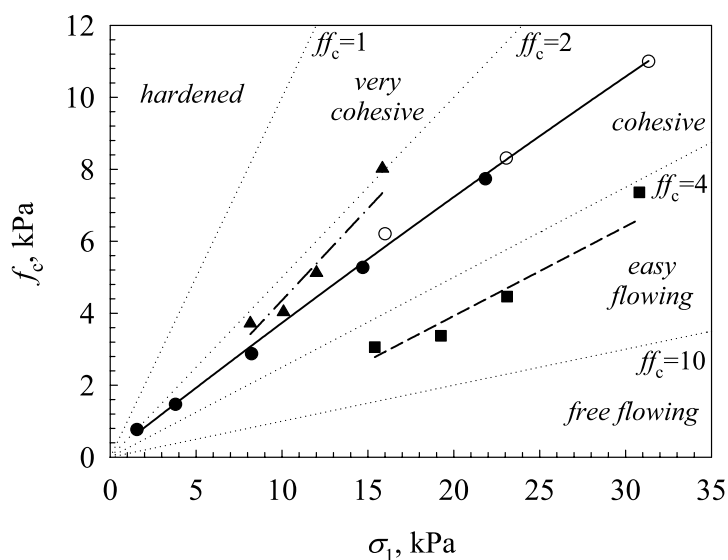

Fig. 7 Flow functions for powder C. ● ○ RST M cell; ○, RST SV10 cell; ■, ideal UCT eqs. (1) and (2); ▲, UCT corrected.

4. Discussion

Significant differences between the flow function results obtained with the RST and the UCT were observed for the more cohesive powders, calcium carbonate, A, B and C. In order to assess whether these discrepancies could be explained by different effective powder compaction values in the two experiments, the UCT results were recalculated taking into account the wall friction and the powder gravitational contribution to the stresses acting in the consolidation step. In support of the hypothesis that the lower consolidation value, which determines the failure load, is attained at the sample bottom, there is the vi-

sual observation that at sample failure, the fracture in the material started at the bottom and then propagated upwards. Resulting flow functions accounting for wall friction and calculated according to Equations (1) and (5) are reported as triangles in **Figs. 4-8**. The re-evaluated UCT flow function is close to the RST flow function for the calcium carbonate powder, suggesting the soundness of the approach followed for UCT flow function correction. Also for powders A, B and C, the re-evaluated UCT flow functions lie very close to those obtained by RST experiments, but only at low consolidation values. For these materials, the corrected UCT flow functions are steeper and more
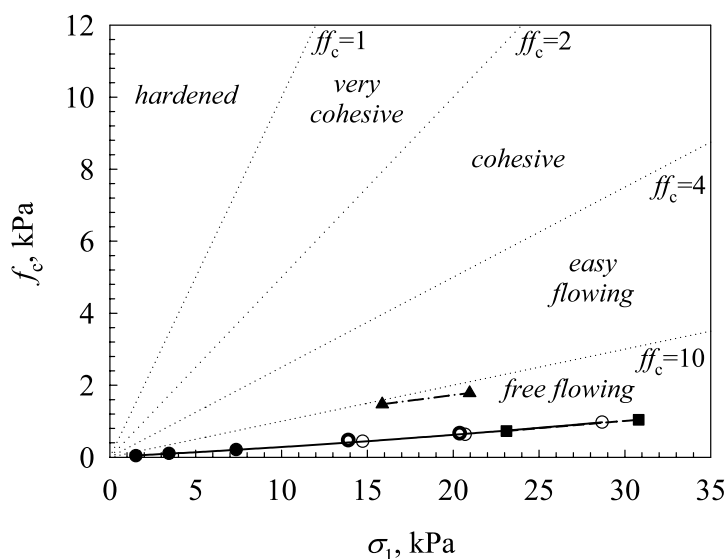
Fig. 8 Flow functions for powder D. ●○ RST M cell; ○, RST SV10 cell; ■, ideal UCT eqs. (1) and (2); ▲, UCT corrected.

linear than the RST flow functions and, therefore, at the higher consolidation values, the RST flow functions provide lower values of the unconfined yield strength. For these powders, other phenomena have to be hypothesized to explain the observed differences at high consolidation levels.

It might be argued that the main reason for obtaining different results between UCT and RST experiments can be attributed to the different stress histories in the sample preparation during the compaction steps for the two testers. In fact, in the RST there is no limit on the maximum shear strain and it is always possible to reach a critical state of deformation in which the powder volume attains a steady value. In the RST procedure, this condition is required to conclude the pre-shearing phase in order to reach a bulk density for a certain compaction load which does not depend on the compaction history. In contrast, the compaction procedure in the UCT does not ensure that the internal deformation of the sample allows the bulk density proper of the critical state to be reached. As a result, it might be expected that under the same major principal stress during compaction, the unconfined yield strength measured with the UCT is somewhat lower than that derived from RST experiments. Nevertheless, as it was recalled in the introduction, experiments carried out by Williams et al. (1971) and by Maltby and Enstad (1993), in which the wall friction was minimized, produced a substantial overlapping of the flow functions obtained with uniaxial testers and the Jenike shear tester. This finding suggests that in these experiments, the internal shearing which occurs in the UCT sample during the

compaction step was sufficient to determine a powder consolidation similar to that obtained with shear testing procedures.

As concerns the present experimental campaign, we have not minimized the wall friction effect in the UCT experiment, but we have accounted for it in the proposed correction of the UCT flow function. Therefore, the circumstance that for powders A, B and C at high consolidation levels, the corrected UCT flow function provides an unconfined yield strength larger than the RST flow function cannot be explained by the occurrence of any significant role of the different stress histories of powder samples in the two experiments. Another possibility is that the high shear induced in the RST might produce some change in the powder structure close to the shear plane such as particle fragmentation or orientation. This interpretation seems to be confirmed by the fact that calcium carbonate, a powder made of rigid particles and not subject to orientation phenomena during shear, does not show significant differences between the RST and the corrected UCT flow function at high consolidation levels. Further preliminary tests on the microscopic structure of the powder on the shear plane did not shed light on this point, and a more complex investigation, which exceeds the scope of this work, would be required.

As concerns the results obtained with powder D, it was observed that the original UCT and RST flow functions were almost identical at all the investigated consolidation levels and the UCT corrected flow function leads to greater unconfined yield strength values. An explanation of this difference with respect

to the other powders tested might be found in the very low compressibility of powder D. This was observed in the consolidation step and was confirmed by the small values of the compressibility index. The consequence might be a reduced powder motion within the cell that might impair the hypothesis of full mobilization of the powder at the container wall during consolidation. This condition is at the base of the Mohr Coulomb approach used to obtain Equation (1) and, if not respected, might lead to an overestimation of the wall friction stress and its effects.

5. Conclusions

A comparison between the ring shear tester and the uniaxial compaction tester techniques for the measurement of powder flow functions was performed for five different powders. Deriving normal stresses simply from the applied external forces, the UCT flow functions gave unconfined yield strengths lower than those measured by the RST for the more cohesive powders, calcium carbonate, A, B and C. In particular, each of these powders resulted in belonging to different flowability regions according to the two techniques. A good agreement between the UCT and RST results was found only for the free-flowing powder D. Recalculation of the stress state of the powder sample in the UCT experiments, taking into account the mould wall friction and the powder weight, gave a flow function in close agreement with that obtained with the RST for the calcium carbonate powder, suggesting the soundness of the approach. For powders A, B and C, the agreement was satisfactory only at low consolidation values. This correction procedure requires knowledge of the K ratio and of the angle of wall friction measurable with shear cells or other testers. As a result, the use of an UCT alone could not be sufficient to measure reliable flow functions unless particular care was taken to eliminate the wall friction effect or at least a rough estimate of the K and wall friction angle of that material was available. **Table 1** suggests that the repose angle for these powders might be a sufficiently good estimate of the effective internal friction to apply equation (2) for estimating K. With cohesive materials, however, which give high angles of internal friction and therefore K values according to equation (2) lower than 0.4, K values equal to 0.4 may provide a fair estimate. For the materials tested, the wall friction angle is approximately half that of the effective internal friction.

It must be recognised, however, that some discrepancies between the RST and the UCT flow functions could not be solved simply taking account of wall friction. In fact at the highest consolidation stresses, the corrected UCT flow functions for cohesive powders (A and B) provide a significantly higher unconfined yield strength of powders. Further investigation is necessary for a better comprehension of this discrepancy.

The proposed correction procedure turns out to be effective to obtain more reliable powder flow functions from simple UCT measurements especially for industrial quality control purposes. Standard shear testers still appear the most reliable and conservative flowability characterization method if the results are to be used for the design of handling or storage equipment such as silos.

List of symbols

A_{RST}	shear cell cross-sectional area	[m^2]
A_{UCT}	UCT mould cross-sectional area	[m^2]
c	cohesion	[kPa]
CI	compressibility index	[-]
D	mould diameter	[m]
d_{32}	Sauter mean size	[μm]
d_{50}	median size	[μm]
f_c	unconfined yield strength	[kPa]
ff_c	flow factor	[-]
g	acceleration due to gravity	[m s^{-2}]
K	ratio between radial and vertical stresses	[-]
M	powder sample weight	[N]
N	external normal force	[N]
N_c	consolidation normal force	[N]
N_f	normal force at failure	[N]
t	time	[s]
z	vertical coordinate	[m]

Greek symbols

Δz	powder height over the shear plane	[m]
μ_w	wall friction coefficient	[-]
φ_e	effective angle of friction	[deg]
φ_i	static angle of friction	[deg]
φ_r	angle of repose	[deg]
φ_w	angle of wall friction	[deg]
ρ_b	powder bulk density	[kg m^{-3}]
σ	normal stress	[kPa]
σ_0	surcharge normal stress	[kPa]
σ_1	major principal stress	[kPa]
τ	shear stress	[kPa]

References

Bell, T.A., Catalano, E.J., Zhong, Z., Ooi, J.Y. and Rotter, J. M. (2007): Evaluation of the Edinburgh Powder Tester,

Proc. of PARTEC 2007, Nuremberg (D), 27-29 March, pap S30_1.

Gerritsen, A.H. (1986): A simple method for measuring powder flow functions with a view to hopper design, Preprint of PARTEC Symposium, Nuremberg (D), 16-18 April 1986, pp.257-279.

Jenike, A.W., (1961): Gravity flow of bulk solids, University of Utah. Utah Engineering. Experiment Station, Bulletin 108.

Kwade, A., Schulze, D. and Schwedes, J. (1994): Determination of the stress ratio in uniaxial compression tests – Part 2, Powder Handling & Processing, 6, pp.199-203.

Maltby, L. P. and Enstad, G., (1993): Uniaxial tester for quality control and flow property characterization of powders, Bulk Solids Handling 13, pp.135-139.

Nedderman, R.M. (1992): "Statics and kinematics of granular materials", Cambridge University Press, Cambridge (UK).

Peschl, I. A. S. Z. (1989): Equipment for the measurement of mechanical properties of bulk materials, Powder Handling & Processing 1, pp.73-81.

Santomaso, A., Lazzaro, P. and Canu, P. (2003): Powder flowability and density ratios: the impact of granules packing, Chem. Eng. Sci., 58, pp.2857-2874.

Schulze, D., (1994): A new ring shear tester for flowability and time consolidation measurements, Proc. of 1st International Particle Technology Forum, Denver (USA), August, pp.11-16.

Schulze, D. (2008): "Powders and Bulk Solids", Springer, Berlin (D).

Schwedes, J. (2003): Review on testers for measuring flow properties of bulk solids, Granular Matter 5, pp.1–43.

Schwedes, J. and Schulze, D. (1990): Measurement of flow properties of bulk solids, Powder Technol. 61, pp.59-68.

Tomas, J. and Schubert, H. (1979): Particle characterisation, Proc. of Partec 79, Nuremberg, Germany, pp. 301-319.

Williams, J.C., Birks, A.H. and Bhattacharya, D. (1971): The direct measurement of the failure function of a cohesive powder, Powder Technol. 4, pp.328-337.

Zhong, Z., Ooi, J.Y. and Rotter, J.M. (2000): Nonlinear effects of blending on coal handling behaviour. Proc. of the 'From powder to bulk', IMechE Conference on Powder and Bulk Solids Handling, London (UK), 13-15 June, pp.17-26.

Author's short biography

Luca Parrella

Luca Parrella is presently design engineer at "Processi Innovativi S.r.l.". After a research stage at PURAC he graduated in Chemical Engineering at the University of Salerno in 2006 with a master level thesis on *"Validation of a simple test method for the rheological properties of food powders"*.

Diego Barletta

Diego Barletta is Assistant Professor of Chemical Engineering at the School of Engineering of the University of Salerno since 2005. He graduated cum laude in Chemical Engineering in 1999 at the University of Napoli Federico II. He obtained the Doctoral degree in Chemical Engineering in 2003 at the University of Salerno. His research activity concerns the use of aeration as a discharge aid of fine powders from storage equipment, the flow properties and the fluidisation behaviour of fine granular materials. In the past, he also worked on modelling combustion and desulphurisation in fluidised bed combustors. He is author of more than 40 papers on refereed international journals and conference proceedings.

Author's short biography

Renee Boerefijn

Renee Boerefijn graduated in 1994 from Twente University in Mechanical Engineering, on the subject of Fluidised Bed Dynamics with Profs. J. J. H. Brouwers and P. Salatino (Naples), and completed a PhD in Chemical and Process Engineering from Surrey University in 1998 on Particle Breakage in Fluidised Bed Jets, under supervision of Prof. M. Ghadiri (Leeds). After this he worked at Unilever Laundry R&D in the roles of Skill Base Leader Granulation, Granulation Project Manager and Group Leader Added Benefit Compounds. Since 2005 with CSM subsidiary PURAC, he now heads the Competence Centre Powders and the Innovation Centre Food & Nutrition. Renee is vice-chair of the technical committee of the International Fine Particles Research Institute (IFPRI), board member of the foundation Ingredients for Food Innovators (IFFI), and member of the EFCE Working Party for Mechanics of Particulate Solids.

Massimo Poletto

Massimo Poletto is associate professor of Chemical Engineering since 2001 at the School of Engineering of the University of Salerno where he is a faculty member of the Department of Chemical and Food Engineering. Presently he is delegate of the Italian Association of Chemical Engineering (AIDIC) to the Working party of the European Federation of Chemical Engineering (EFCE) on "Mechanics of Particulate Solids" where is was elected chairman for the period 1/1/2008-31/12/2010. Massimo Poletto is author of more than 100 papers and conference presentations, more than 30 of which have been published on refereed international Journals in the field of fluidization powder mechanics and food technology applications of chemical engineering.